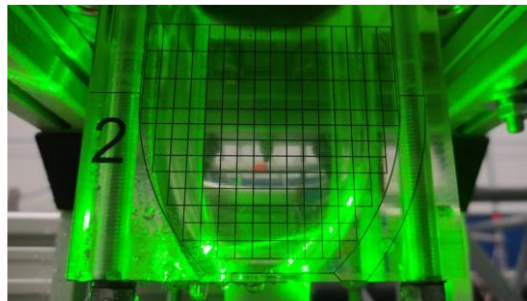


# Laser Doppler Anemometry technique to study the flow field in the nozzle and in the water jet of a Pelton turbine

Giuseppe Roberto Pisaturo<sup>1</sup>, Francesco Fabio Nicolosi<sup>1</sup>, Daniele Gusmerotti<sup>1</sup>, Maurizio Righetti<sup>1</sup> and Massimiliano Renzi<sup>1\*</sup>

<sup>1</sup>Free University of Bozen/Bolzano, Faculty of Science and Technology, 39100 Piazza Università 5, Bolzano, Italy

**Abstract.** The constant availability of water from the mountain basins is crucial to feed the hydropower plants that represent currently the most important renewable energy source in many countries, like Italy. The long dry periods that are nowadays registered during the summer periods have imposed the managers of the hydropower plants to operate the machines at very low flow rates, close to the lowest allowed values. In this work we focus our attention on the fluid-dynamics of the water jet of a Pelton machine and of the corresponding nozzle, with particular attention to the low flow-rate ranges. The nozzle has been manufactured in PMMA to be able to study the internal fluid-dynamics using the Laser Doppler Anemometry (LDA) technique. The shape of the nozzle has been adapted to limit the laser beam distortion and an algorithm has been implemented to correct the position of the measurement volume and the evaluation of the velocity components. Moreover, a specific measurement layout has been proposed and implemented to be able to study the velocity of the water jet downstream the nozzle and to study the homogeneity of the flow velocity in the jet, which is a crucial characteristic to grant a proper operation of the Pelton runner. The specific set-up of the test bench and the LDA parameters are presented; the signal of the LDA receiver proved to be very consistent and reliable. Moreover, the results of the measurements have been used to validate CFD simulations and to extend the results of the analyses to other operating conditions of the Pelton nozzle.



## Nomenclature

CFD	Computational Fluid Dynamic
LDA	Laser Doppler Anemometry
PLC	Programmable Logic Controller
PMMA	Poly Methyl Methacrylate.
RES	Renewable Energy Source

## 1 Introduction

Increasing the share of Renewable Energy Sources (RES) in the electricity production is mandatory to cope with the emission reduction goals set by many countries to reduce the greenhouse gases emissions. Currently, in the electricity production, RES accounted for the 28.3% by the end of 2021 [1]; in particular, hydropower contributed with a share of 15%. Even though new

hydropower plants are still build in few places in Asia [2], due to the developing of other RES technologies and to the almost total exploitation of available waterpower sites, this piece of data is continuously decreasing. Hydropower rotors, such as Pelton [3], [4], Francis [5], [6] and Kaplan [7], [8], are designed according to the values of hydropower plant's flow rate and hydraulic head.

Focusing the attention on Pelton machines, this is an action hydraulic turbine characterized by low values of specific speed since it exploits low flow rates and high heads. The water arrives inside the nozzles through a distributor, which splits the water flow according to the number of nozzles. Then, the water impinges on buckets located on the rotor periphery. Each nozzle has a spear valve that can slide axially to regulate the flow rate exiting from the nozzle, thus providing the water with

---

\* Corresponding author: [massimiliano.renzi@unibz.it](mailto:massimiliano.renzi@unibz.it)

the best momentum exchange when it impinges on the buckets.

Because of climate changes, in some locations of the globe in summer periods the lack of water compromises Pelton rotor performance since the efficiency quickly decreases when operating at strong part-load conditions, typically below 30% of the nominal flow rate.

Several CFD studies have been performed on Pelton nozzle design to study secondary flows and improve the water jet quality. Chongji and al. [9] performed numerical simulations on a 3D Pelton nozzle investigating the external flow using three different spear strokes. The results showed that the higher is the nozzle opening, the higher is the dispersion of the water jet, thus leading to higher hydraulic losses and poor performance of the Pelton bucket. Zhang et al. [10] performed a CFD simulation with a spear angle of  $70^\circ$  achieving higher efficiency values compared to the standard  $50^\circ$ - $60^\circ$ . Petley et al. [11] experimented and simulated how the nozzle and spear valve configuration affect the performance of a Pelton turbine. Even though numerical simulations showed higher performance in injector with notably steeper nozzle, experimental data suggested that an upper limit appears beyond which steeper angles designs are no longer optimal. Kumashiro et al. [12] performed numerical and experimental investigation on a Pelton turbine focusing the attention on unsteady flow patterns around the bucket, which depend on water-jet non uniformity due to the secondary flows mainly created by the distributor, spear valves bending pipes together with their supports upstream.

Zhang and al. [13] experimentally investigated the secondary flow structure of a free surface Pelton jet flow using a two-component Laser Doppler Anemometry (LDA) together with a small wedge of Plexiglas varying the head from 10 m to 30 m. In the free surface, secondary flows deviate from the stagnation point and can deform the jet surface.

Though several CFD simulations and numerical studies have been performed by scientists, there is a lack of experimental data regarding the measurement of the velocity contour and velocity homogeneity of the water flow in the nozzle and in the water jet, downstream the nozzle. This is also due to the complexity of accurately measuring the flow velocity through traditional techniques and without affecting the water jet fluid dynamics. Therefore, the aim of this work is to characterize the velocity profile of a nozzle and of the free wall jet of a Pelton distributor when the turbine operates in low flow-rate conditions. A specific experimental set-up and a measurement technique, based on LDA, has been developed for this purpose.

## 2 Methods

### 2.1 Experimental setup

The experimental plant is located in the Fluid Dynamic Lab of the Free University of Bozen/Bolzano and consists of a Rovatti SN3E65-250-E-GR-TM-SS pump with a maximum head of 20 m controlled by a PLC

system and a circuit to connect the pump to the nozzle (Fig. 1).



**Fig. 1** Set-up for LDA measurement of the water speed. The following can be distinguished: 1 Supply pipe, 2 Pelton nozzle, 3 Laser emitter, 4 Drive traversing system.

The model of the Pelton nozzle is made of Poly-methyl methacrylate (PMMA) and has been manufactured from the company Troyer S.p.A (Fig. 2). This material is particularly apt for the use with LDA technique for its optical transparency, properties, and stability. The nozzle is characterized by three walls having a flat outer surface perpendicular to the ground, and one wall having a surface that instead follows the inner contour of the nozzle (Fig. 2). These two different configurations were designed to assess the effect of the optical distortion caused by a curved surface crossed by the laser light. The presence of a curved surface deforms and shifts the position of the measurement volume and, therefore, has to be carefully evaluated when running an LDA measurement. The diameter of the nozzle in the cylindrical section is 81.5mm, while the nozzle exit section is 36 mm.

The measurements were conducted considering a flow rate of 14 l/s and a head of 18 m. This flow rate is about 35% of the nominal flow rate of the nozzle since, as stated in the introduction, it is of great interest to analyze the behavior of the nozzle in the low flow rate region.

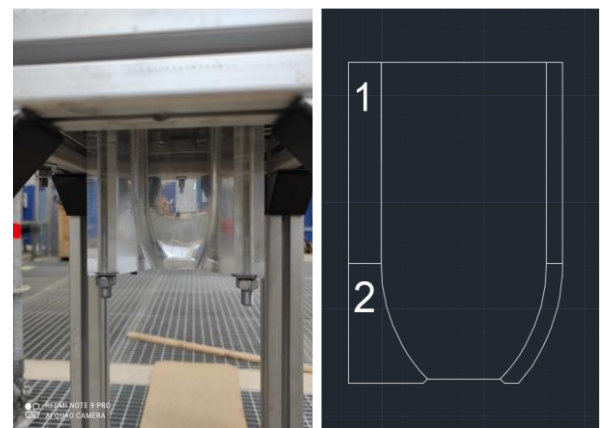


**Fig. 2** Detail (left) and sketch (right) of the prototype Pelton nozzle.

The use of a transparent nozzle to study the internal flow field does not allow to run the tests at high pressure. It would be instead possible to study the water jet downstream the nozzle also at high pressure with the set-up and the solutions described hereinafter for the LDA technique.

## 2.2 Measuring technique

An LDA emitter from Dantec Dynamic was used, with two pairs of laser beams (wavelength of 532 nm for the first velocity component and 561 nm for the second velocity component) incident on each other (focal length 300mm), to define a control volume within which water velocity measurements are taken. The maximum laser power is 300 mW for each pair of laser beams. Signal processing was carried out with the Dantec Dynamics Burst Spectrum and a dedicated Dantec software (BSA Flow Software).

### 2.2.1 Measurements in the Pelton nozzle

The LDA emitter is mounted on a rotating support, and it is moved by a traverse system, which allows it to move it along two planes: horizontal (perpendicular to the symmetry axis of the nozzle) and vertical (parallel to the symmetry axis of the nozzle) (Fig. 3).

The sampling frequency was always between 100 Hz and 200 Hz (depending on the measuring point), and 20,000 velocity measurements were collected for each measurement point. This amount of data ensured a negligible sampling error and the possibility to calculate the time averaged velocity correctly.

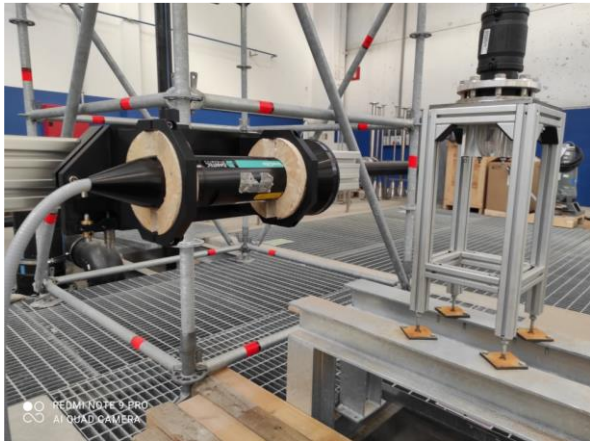


**Fig. 3** Dantec Dynamic LDA emitter, nozzle, and rotating support.

A grid of volumes was defined within the nozzle at which the velocity measurements were to be taken (**Errore. L'origine riferimento non è stata trovata.**).

The axis of symmetry of the jet and a radial axis 15 mm above the demarcation surface between the nozzle's constant-section volume (Part 1 in Fig. 4) and the variable-section volume (Part 2 in Fig. 4) were taken as reference axes. The point of intersection of these two axes was taken as the origin of the grid, having position (0,0). From this point onwards, several velocity measurements were taken, moving 5 mm along the

horizontal axis (r-axis) and 10 mm along the vertical axis (z-axis).

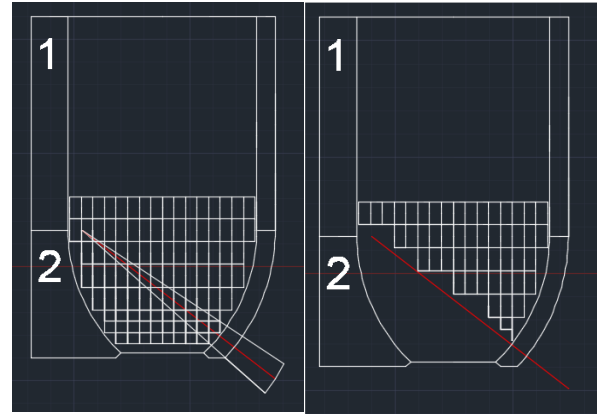


**Fig. 4** Side view of measuring grid for the Pelton nozzle (left) and identification of the measurement limits, with the limit position in red (right).

To improve the signal-to-noise ratio, it was decided to use two different approaches for the receiving optic positioning. For Part 1, the emitter is positioned to the surface, and it was used the backscatter technique in which the receiver is mounted inside the emitter. For the Part 2, using the rotating support, the emitter is positioned so that it is always perpendicular to the tapered surface of the nozzle, so that the effect of the wall on refraction is constant. The receiver was looking at the measuring volume at an angle (off-axis scattering). This choice was made to reduce the sensitivity to velocity gradients within the measuring volume and therefore reduce problems with reflection. Nevertheless, the use of off-axis scattering requires a separate receiver and thus involved careful alignment with the emitter. To ensure the maximum signal quality, the receiver was gently moved approaching the sampling volume and signal was monitored with the BSA Flow Software. When the signal quality was the higher possible, it was assumed that the receiver was well positioned.

Adopting this technique, it was not possible to plot the final portion of the nozzle, as can be seen in Fig. 4. It was possible to trace the value of some measuring points, adopting the axisymmetric casting hypothesis (Fig. 5).

The laser beams from the emitter pass through three different materials before forming the measurement volume. These materials are air, the PMMA that constitutes the Pelton's nozzle and finally the water contained within it and the object of measurement. Since the laser beams from the emitter always result slightly inclined with respect to the passing surfaces, their transmission from one medium to another is linked to the change in direction in the propagation of light. To take this phenomenon into account, the law of refraction, also known as Snell's law, was used to make corrections to the correct positioning of emitter source and the value of the measured velocity [14].



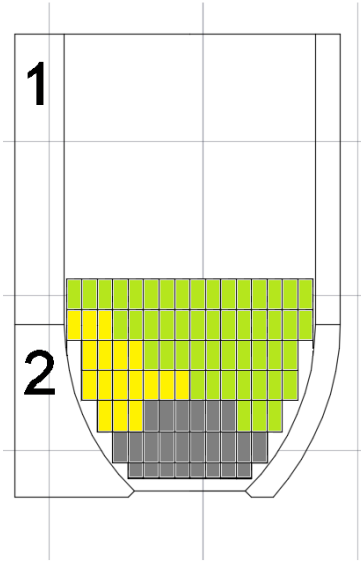


**Fig. 5** Definition of the 'measurable zone' (green) and 'blind zone' (grey) and additional grid positions that can be estimated with the axisymmetric assumption (yellow).

Let's consider the scheme in Fig. 6. To obtain the segment  $AB$ , that it is the distance between the emitter source and the outer PMMA wall of the Pelton nozzle, is necessary to follow the following steps:

1. Calculate the  $\alpha_1$  angle

$$\alpha_1 = \arctan(MA/AD)$$

where  $MA$  is half of the distance between the two lasers at the emitter (14.14 mm) and  $AD$  is the focal length (310 mm);

2. Calculate the  $\alpha_2$  angle applying the Snell's law

$$\alpha_2 = \arcsin_{PMMA} \left( \frac{n_{air}}{n_{PMMA}} \cdot \sin(\alpha_1) \right)$$

where  $n_{air}$  and  $n_{PMMA}$  are the refractive index of air and PMMA, respectively;

3. Calculate  $\alpha_3$

$$\alpha_3 = \arcsin_{water} \left( \frac{n_{PMMA}}{n_{water}} \cdot \sin(\alpha_2) \right)$$

where  $n_{water}$  is the water refractive index;

4. Calculate the segment  $GC$ ,  $HI$ ,  $ML$  and finally  $AB$

$$GC = CF \cdot \tan(\alpha_3)$$

$$HI = BC \cdot \tan(\alpha_2)$$

$$ML = MA - (HI + GC)$$

$$AB = ML / \tan(\alpha_1)$$

where  $CF$  is half of the nozzle inner diameter (40.75 mm).

To take measurements also in the blinded zone it was decided to put the laser source on the flat outer surface of the Pelton nozzle trying to match the points following the same approach for Part 2 (Fig. 7).

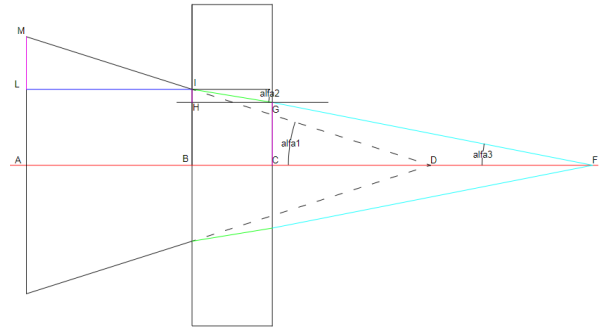


**Fig. 6** Optical scheme to calculate the refractions through different media.

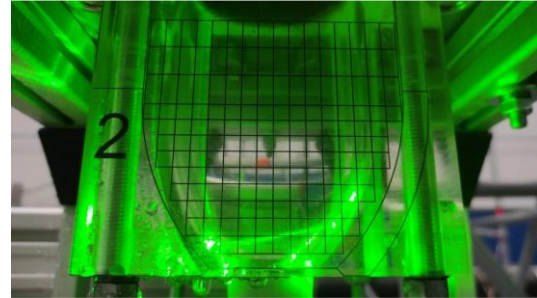


**Fig. 7** Laser speed measurement in the blind nozzle area with the help of the transparent template

## 2.2.2 Measurements in the water jet

A slider consisting of a rectangular PMMA parallelepiped was used to measure the velocity field inside the water jet, downstream the nozzle. The slider, capable of being moved by two micrometer screws, is intended to gain optical access to the inside of the jet, thus creating an optical window. The slider was then positioned so that it lapped the water jet without causing a disturbance in the velocity field in the area beyond its axis of symmetry (area where measurements were made) (Fig. 8). Vertically, the slider was positioned at one diameter from the Pelton nozzle, to avoid the region in which the jet contraction is present. The sample points were positioned every 1 mm from the jet axis to the outer jet surface (Fig. 9). It was decided to take the velocity measurements in the half of the jet furthest from the slider to minimise any disturbances introduced by the slider presence.

The measurements were carried out using LDA technique in backscatter acquiring with a sampling frequency between 100 Hz and 200 Hz, and 20,000 velocity measurements were collected for each measurement point.

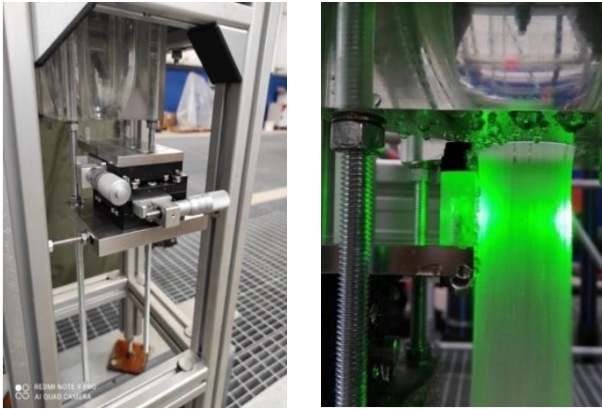


**Fig. 8** Slider support and photo of the proposed measurement technique for the water jet.

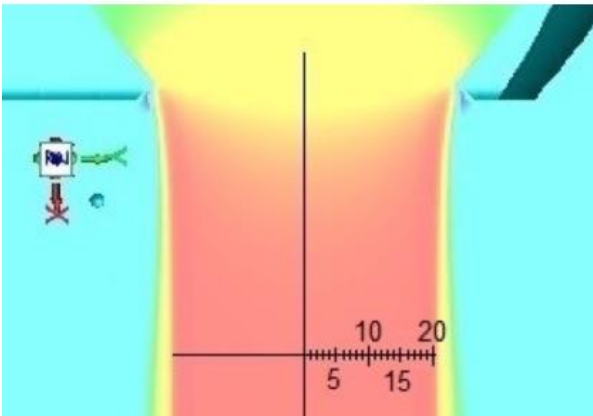


**Fig. 9** Reference system for the velocity measurements in the water jet. The numbers 1-20 represent the measurement points.

### 3 Results

#### 3.1 Velocity field in the Pelton nozzle

The table in Fig. 10 reports the results obtained in the measurement of the water axial velocity field in the PMMA nozzle. As expected, close to the lateral walls the velocity tends to decrease because of the presence of the boundary layer. The effect of the boundary layer is more intense in the upper zone (constant section) because of the lower velocity of the flow and a velocity gradient is clearly visible. A slight asymmetry flow field can also be noticed probably because of the presence of a bend upstream the nozzle, which can cause secondary flows. The numbers in blue colour represent those velocity values that could not be directly measured because of optical limitations and that were assumed according to an axis-symmetric assumption of the flow; therefore, the accuracy of these values is lower.

In the converging section of the nozzle the velocity obviously increases, coherently with the reduction of the section. Also, in this case it is possible to notice the lower velocity of the flow close to the lateral surface and the average water speed is coherent with the mass flow rate conservation. Unfortunately, it was not possible to reach the very last part of the nozzle with the laser rays

because of the optical distortion of the beams and the lack of a proper optical interface.

MAPPATURA VELOCITA' UGELLO																				
	-40	-35	-30	-25	-20	-15	-10	-5	0	5	10	15	20	25	30	35	40			
0	0.9	1.1	1.0	1.0	1.4	1.6	1.6	1.6	1.7	1.6	1.7	1.8	1.8	1.8	1.7	1.6	0.1			
-10	0.3	0.7	0.9	1.4	1.6	1.7	1.7	1.8	1.8	1.8	1.9	1.9	1.8	1.9	2.3	0.2	0.2			
-20	0.5	0.9	0.9	1.3	1.7	1.9	2.1	2.1	2.2	2.2	2.2	2.3	2.3	2.3	0.9	0.9	0.5			
-30	5.0	5.9	6.0	6.2	6.3	6.4	6.5	6.5	6.5	6.5	6.5	6.4	6.3	6.2	6.0	5.9	5.0			
-35	5.0	6.0	6.0	6.4	6.1	6.3	6.5	6.5	6.6	6.5	6.5	6.3	6.1	6.4	6.0	6.0	5.0			
-40	6.1	6.3	6.4	6.4	6.5	6.6	6.7	6.7	6.7	6.7	6.6	6.5	6.4	6.4	6.3	6.1				
-45	5.1	5.9	6.4	6.5	6.7	6.8	7.0	7.1	7.0	6.8	6.7	6.5	6.4	5.9	5.1					
-50	5.1	6.4	6.7	6.6	6.8	7.0	7.1	7.2	7.1	7.0	6.8	6.6	6.7	6.4	5.1					
-55		6.2	6.7	6.9	7.3	7.2	7.2	7.3	7.2	7.2	7.3	6.9	6.7	6.2						
-60		6.0	6.7	7.1	7.3	7.9	8.1	7.3	8.1	7.9	7.3	7.1	6.7	6.0						
-65			7.7	7.4	8.0	8.4	8.8	9.2	8.8	8.4	8.0	7.4	7.7							

**Fig. 10** Mapping average speeds for all measurements made in the measurement grid

#### 3.2 Velocity measurement in the water jet

Fig. 11 shows the axial velocity trend for all the positions of the measurement axis (see Fig. 9) at a distance of one diameter downstream the exit of the nozzle. Point 1 refers to the axis of the jet, while point 21 is located on the external edge of the jet. In general, the average flow velocity is consistent with the mass flow rate conservation, also considering the nozzle losses, and it confirms the accuracy of the proposed measurement technique. As can be seen from the trend line in red, the jet velocity decreases as it moves away from the centre of the jet, consistent with what is defined in the literature [14]. The velocity tends to be slightly higher in the center of the nozzle, as expected because of the absence of the spear valve. The axial velocity remains however quite constant also at the outer edge of the jet confirming the good quality of the formed water jet. This will imply also a favourable operating condition for the buckets of a Pelton runner.

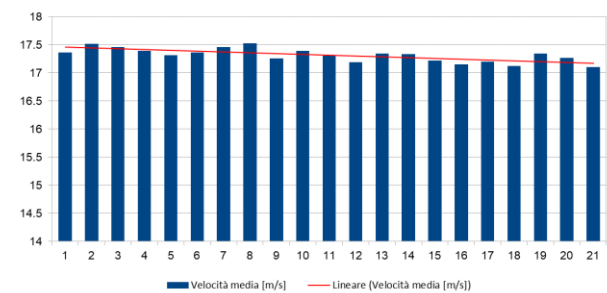


**Fig. 11** Trend of average velocities along the jet axis in the 20 selected measurement points (see Fig. 7).

### 4 Conclusions

The work presents a methodology to perform velocity field measurements in complex geometries like the case of a Pelton turbine nozzles. The use of the Laser Doppler Anemometry (LDA) technique has the advantage of being non-intrusive and of being able to obtain a large number of samples for each measurement point.

Thanks to the measurements made it was possible to obtain the velocity field inside the nozzle and also inside the jet leaving the same nozzle. This latter requires a specific solution to create an optical window for the laser beams. The proposed methodology required an a posteriori optical correction for the correct

determination of the position of the measuring volume and the value of the measured velocity, caused by the presence of non-flat surfaces. The results show that inside the nozzle, as expected, the minimum velocity is located close to the walls. A velocity profile in the nozzle can be recorded, which is consistent with the expected theoretical values. Regarding the velocity field inside the jet, the axial velocity remains quite constant till the outer edge of the jet confirming the good quality of the formed water jet.

The activities were conducted as part of the Turb-Hydro project that also involved the company Troyer S.p.A. in Sterzing – Vipiteno (BZ).

## References

- [1] REN21, *Renewables 2022*. 2022.
- [2] L. Liu *et al.*, “Quantifying the potential for reservoirs to secure future surface water yields in the world’s largest river basins,” *Environ. Res. Lett.*, vol. 13, no. 4, 2018, doi: 10.1088/1748-9326/aab2b5.
- [3] R. MacK, B. Gola, M. Smertnig, B. Wittwer, and P. Meusburger, “Modernization of vertical Pelton turbines with the help of CFD and model testing,” *IOP Conf. Ser. Earth Environ. Sci.*, vol. 22, no. January, 2014, doi: 10.1088/1755-1315/22/1/012002.
- [4] N. Kholifah, A. C. Setyawan, D. S. Wijayanto, I. Widiastuti, and H. Saputro, “Performance of Pelton Turbine for Hydroelectric Generation in Varying Design Parameters,” *IOP Conf. Ser. Mater. Sci. Eng.*, vol. 288, no. 1, 2018, doi: 10.1088/1757-899X/288/1/012108.
- [5] K.-R. G. Jakobsen and M. A. Holst, “CFD simulations of transient load change on a high head Francis turbine,” *J. Phys. Conf. Ser.*, vol. 755, no. 1, 2016, doi: 10.1088/1742-6596/755/1/011001.
- [6] F. Pochylý, P. Rudolf, D. Štefan, P. Moravec, J. Stejskal, and A. Skoták, “Design of a pump-turbine using a quasi-potential flow approach, mathematical optimization and CFD,” *IOP Conf. Ser. Earth Environ. Sci.*, vol. 240, no. 7, 2019, doi: 10.1088/1755-1315/240/7/072043.
- [7] L. Motycak, A. Skotak, and J. Obrovsky, “Analysis of the Kaplan turbine draft tube effect,” *IOP Conf. Ser. Earth Environ. Sci.*, vol. 12, p. 012038, 2010, doi: 10.1088/1755-1315/12/1/012038.
- [8] A. Rivetti, C. Lucino, S. Liscia, D. Muguerza, and F. Avellan, “Pressure pulsation in Kaplan turbines: Prototype-CFD comparison,” *IOP Conf. Ser. Earth Environ. Sci.*, vol. 15, no. PART 6, 2012, doi: 10.1088/1755-1315/15/6/062035.
- [9] Z. Chongji *et al.*, “Numerical Analysis of Pelton Nozzle Jet Flow Behavior Considering Elbow Pipe,” *IOP Conf. Ser. Earth Environ. Sci.*, vol. 49, no. 2, 2016, doi: 10.1088/1755-1315/49/2/022005.
- [10] J. Zhang *et al.*, “Optimal design of a pelton turbine nozzle via 3D numerical simulation,” *IOP Conf. Ser. Earth Environ. Sci.*, vol. 163, no. 1, 2018, doi: 10.1088/1755-1315/163/1/012066.
- [11] S. Petley *et al.*, “Investigating the influence of the jet from three nozzle and spear design configurations on Pelton runner performance by numerical simulation,” *IOP Conf. Ser. Earth Environ. Sci.*, vol. 240, no. 2, 2019, doi: 10.1088/1755-1315/240/2/022004.
- [12] T. Kumashiro *et al.*, “Numerical investigation of the jet velocity profile and its influence on the Pelton turbine performance,” *IOP Conf. Ser. Earth Environ. Sci.*, vol. 240, no. 7, 2019, doi: 10.1088/1755-1315/240/7/072006.
- [13] Z. Zhang and M. Casey, “Experimental studies of the jet of a Pelton turbine,” *Proc. Inst. Mech. Eng. Part A J. Power Energy*, vol. 221, no. 8, pp. 1181–1192, 2007, doi: 10.1243/09576509JPE408.
- [14] Z. Zhang, *LDA Application Methods - Laser Doppler Anemometry for Fluid Dynamics*, vol. 36. 2010. [Online]. Available: <http://www.ncbi.nlm.nih.gov/pubmed/22928395>.